



Moabite, NiFe³⁺(PO₄)O, a new natural oxyphosphate

Sergey N. Britvin^{1,2}, Mikhail N. Murashko¹, Maria G. Krzhizhanovskaya¹, Yevgeny Vapnik³,
Natalia S. Vlasenko¹, Oleg S. Vereshchagin¹, Dmitrii V. Pankin¹, and Evgeny A. Vasiliev⁴

¹Saint Petersburg State University, Universitetskaya Emb. 7/9, St Petersburg 199034, Russia

²Nanomaterials Research Centre, Kola Science Centre, Russian Academy of Sciences,
Apatity 184209, Russia

³Department of Earth and Environmental Sciences, Ben-Gurion University of the Negev,
P.O. Box 653, Beer-Sheva 84105, Israel

⁴Saint Petersburg Mining University, 2, 21st Line, St Petersburg 199106, Russia

Correspondence: Sergey N. Britvin (sergei.britvin@spbu.ru)

Received: 28 January 2025 – Revised: 20 March 2025 – Accepted: 24 March 2025 – Published: 17 June 2025

Abstract. Moabite, NiFe³⁺(PO₄)O, is a new natural oxyphosphate discovered in pyrometamorphic rocks of the Daba-Siwaqa complex, a subdivision of the Hatrurim Formation in central Jordan. The mineral is named for the Kingdom of Moab, an ancient state that existed on the territory of the modern Jordan. Moabite is an accessory phase in the phosphide–phosphate assemblages, where it associates with diopside; anorthite; crocobelonite, CaFe³⁺(PO₄)₂O; yakubovichite, CaNi₂Fe³⁺(PO₄)₃; hematite; negevite, NiP₂; murashkoite, FeP; transjordanite, Ni₂P; halamishite, Ni₅P₄; native iron (α -Fe); and an alluaudite-group phosphate whose composition is exactly midway between the two endmembers NaNaCa(Fe³⁺Mg)(PO₄)₃ and \square NaCa(Fe³⁺Fe³⁺)(PO₄)₃. The mineral forms isometric to short prismatic crystals and euhedral grains up to 30 μ m across. Macroscopically, it has a deep-brown colour. In the polished sections in transmitted light, the mineral is translucent red-brown. It has a Mohs hardness rating of 4. Cleavage was not observed. The density, 4.324 g cm⁻³, was calculated based on the empirical formula and unit-cell parameters obtained from single-crystal refinement. The chemical composition was as follows (electron microprobe, wt %): NiO 29.75, CuO 1.73, MgO 0.45, Fe₂O₃ 36.04, Al₂O₃ 0.19, Cr₂O₃ 0.18, V₂O₅ 0.47, P₂O₅ 31.22, total 100.03. The empirical formula calculated on the basis of 5 oxygen atoms per formula unit (apfu) is (Ni_{0.90}Cu_{0.05}Mg_{0.03})_{Σ0.98}(Fe³⁺_{1.01}Al_{0.01}Cr_{0.01})_{Σ1.03}(P_{0.99}V⁵⁺_{0.01})_{Σ1.00}O₅, corresponding to the ideal NiFe³⁺(PO₄)O. Moabite is orthorhombic; the space group is *Pnma* (no. 62); and *a* = 7.2161(16), *b* = 6.4064(15), *c* = 7.4706(19) Å, *V* = 345.4(1) Å³ and *Z* = 4. The strongest lines of X-ray powder diffraction pattern are as follows [*d* in Å (I) (hkl)]: 5.20(63)(101), 3.321(37)(102), 3.251(83)(201), 2.7262(100)(121), 2.5946(37)(202), 2.3542(25)(103) and 2.3044(24)(122). The crystal structure has been solved and refined to *R*₁ = 0.033 for 389 unique observed reflections. Moabite is the first mineral that crystallizes in the α -Fe₂PO₅ (α -Fe₂OPO₄) structure type. It has a direct synthetic analogue, and it is isotopic to antiferromagnetic transition metal oxyphosphates of the general formula *A*²⁺*B*³⁺OPO₄, where *A*²⁺ = Fe, Ni, Co and Cu and *B*³⁺ = Fe, V and In.

1 Introduction

The Hatrurim Formation, a large complex of pyrometamorphic rocks in the Middle East (Gross, 1977), is distinguished by the unprecedented diversity of phosphorus-bearing minerals. They include a palette of silicophosphates and carbonate phosphates (Galuskin et al., 2015, 2016, 2018a, b,

2019, 2021; Sokol et al., 2015), anhydrous orthophosphates (Britvin et al., 2021c, 2023b; Galuskin et al., 2023a, 2024; Juroszek et al., 2023; Krzatała et al., 2023), phosphides (Britvin et al., 2015, 2020a, b, c, 2021b, 2022a; Murashko et al., 2022; Galuskin et al., 2023b), condensed phosphates (Britvin et al., 2021d), and oxyphosphates (Galuskin et al., 2018b, 2021; Britvin et al., 2023a). The majority of these

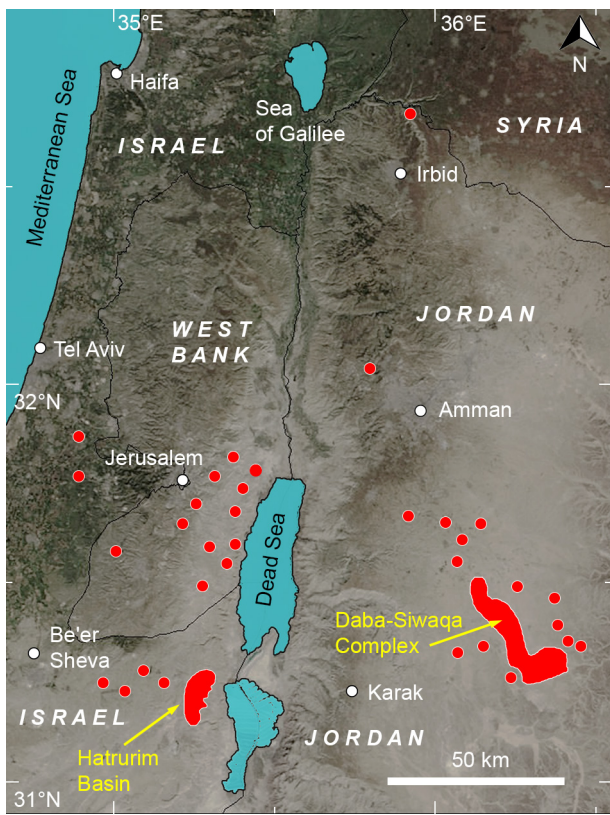


Figure 1. Location of the Hatrurim Formation outcrops across the territory of the southern Levant. The largest massif is a Daba-Siwaqa complex in Jordan. Adapted from Britvin et al. (2021d) (CC-BY license).

minerals are endemic, reflecting the unique and still controversially interpreted processes that triggered the emergence of the formation (Gross, 1977; Burg et al., 1992; Fleurance et al., 2013; Sokol et al., 2007, 2010, 2012; Novikov et al., 2013; Britvin et al., 2021a, 2022b, c, d). In this paper we focus on a specific subset of phosphate minerals, pure oxyphosphates, which are characterized by (1) an anhydrous composition, (2) the presence of a so-called “additional” oxygen atom in their chemical formulas and (3) the absence of other anions. These oxyphosphates are now comprised by six terrestrial species and two minerals of meteoritic origin (Table 1). We herein present a description of moabite, $\text{NiFe}^{3+}(\text{PO}_4)\text{O}$, a new representative of natural oxyphosphates. The mineral is named for the Kingdom of Moab, an ancient state that emerged in the late 10th century to 11th century BCE on the territory of the modern Hashemite Kingdom of Jordan (e.g. Finkelstein and Lipschits, 2011). The holotype specimen of moabite is deposited in the collections of the Fersman Mineralogical Museum of the Russian Academy of Sciences, Moscow, Russia, with the registration number 5627/1.

2 Samples and methods

Electron microprobe analysis was conducted on the polished carbon-coated thin sections, using a WAVE 500 wavelength-dispersive spectrometer (Oxford Instruments) attached to a Hitachi S-3400 N scanning electron microscope. The spectrometer was operated at an acceleration voltage of 20 kV, beam current of 15 nA and beam diameter of 2 μm . The following standards and $K\alpha$ lines were used: diopside (Mg), trevorite (Ni), Cu metal (Cu), hematite (Fe), gehlenite (Al), V metal (V), Cr metal (Cr) and chlorapatite (P). The same polished sections were used for subsequent spectroscopic studies after the removal of carbon film. *Optical reflectance* data were acquired by means of a Leica DM4500P microscope and TIDAS E MSP spectrophotometer calibrated against the Si standard.

The *Raman spectrum* was obtained by means of a LabRAM HR800 (HORIBA Jobin Yvon) spectrometer equipped with an Olympus microscope, 50 \times confocal objective and He–Ne laser ($\lambda = 632.8 \text{ nm}$). *X-ray single-crystal data* were collected using a Bruker Kappa APEX DUO Diffractometer (CCD detector, charge-coupled device), equipped with a microfocus tube (Mo $K\alpha$ radiation). The crystal structure was solved and refined using the SHELX-2018 set of programs (Sheldrick, 2015) embedded into the Olex2 graphical user interface (Dolomanov et al., 2009). Data collection and structure refinement details are summarized in the section on crystal structure. Full crystallographic information can be retrieved from the crystallographic information file (CIF) attached to the Supplement. *X-ray powder diffraction data* were obtained by means of a Rigaku RAXIS Rapid II diffractometer (semi-cylindrical imaging plate, Debye–Scherrer geometry, $r = 127.4 \text{ mm}$), under the following conditions: Co $K\alpha$ radiation (rotating anode with microfocus tube), 40 kV, 15 mA and 60 min exposure. Conversion of the image plate to the profile and processing were carried out using the ocs2xrd program (Britvin et al., 2017) and Stoe WinXPOW v2.03 (Stoe & Cie GmbH, Darmstadt, Germany).

3 Occurrence

The geological setting of the Hatrurim Formation is described in numerous reports and reviews (Gross, 1977; Burg et al., 1992; Fleurance et al., 2013; Novikov et al., 2013; Abzalov et al., 2015; Sokol et al., 2019; Vereshchagin et al., 2024b). In brief, the formation, also known as “the Mottled Zone”, is comprised of dozens of rock outcrops exposed on both the Jordanian and Israeli sides of the Dead Sea, with some patches traced far north along the Jordan River (Fig. 1). The spread of the Mottled Zone outcrops coincides with the area affected by the tectonics of the Dead Sea transform fault system (Ben-Avraham et al., 2008). The age dating of the pyrometamorphic event(s) gives controversial results, from 16 Ma to even $\sim 250 \text{ ka}$ (e.g. Sokol et al.,

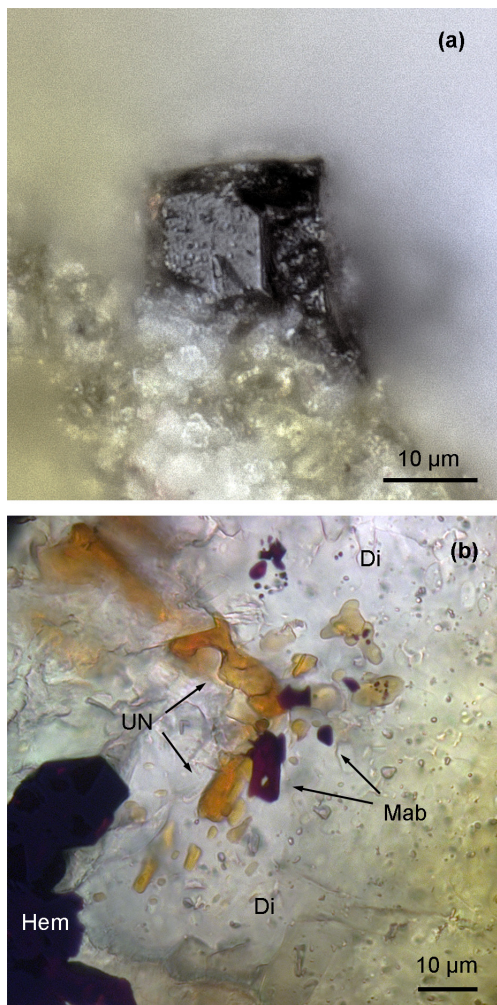
Table 1. Oxyphosphate minerals with no other additional anions.

Mineral	Formula	Origin*	Reference
Moabite	$\text{NiFe}^{3+}(\text{PO}_4)\text{O}$	T	This work
Staněkite	$\text{Mn}^{2+}\text{Fe}^{3+}(\text{PO}_4)\text{O}$	T	Keller et al. (1997)
Joosteite	$\text{Mn}^{2+}\text{Mn}^{3+}(\text{PO}_4)\text{O}$	T	Keller et al. (2007a)
Grattarolaite	$\text{Fe}_3^{3+}(\text{PO}_4)_3\text{O}$	T	Cipriani et al. (1997)
Crocobelonite	$\text{CaFe}_2^{3+}(\text{PO}_4)_2\text{O}$	T	Britvin et al. (2023a)
Beershevaite	$\text{CaFe}_3^{3+}(\text{PO}_4)_3\text{O}$	T	IMA 2020-095a
Elaliite	$\text{Fe}_8^{2+}\text{Fe}^{3+}(\text{PO}_4)_8$	M	Herd et al. (2024)
Elkinstantonite	$\text{Fe}_4^{2+}(\text{PO}_4)_2\text{O}$	M	Herd et al. (2024)

* Origin: terrestrial (T) or meteoritic (M).

Table 2. Reflectance values of moabite measured in air (%).

R_{\max}	R_{\min}	λ (nm)	R_{\max}	R_{\min}	λ (nm)
14.0	14.0	420	13.1	12.9	580
14.4	14.4	440	13.1	12.9	589
14.0	13.8	460	13.0	12.8	600
14.1	14.0	470	12.9	12.6	620
14.3	14.1	480	12.8	12.7	640
14.3	14.0	500	12.8	12.7	650
13.9	13.7	520	12.8	12.7	660
13.6	13.3	540	12.8	12.6	680
13.5	13.3	546	13.1	12.9	700
13.3	13.1	560	13.5	13.4	720

**Figure 2.** (a) Moabite crystal in an anorthite–diopside matrix. (b) Thin section of the paralava containing moabite (Mab), unnamed alluaudite-group phosphate (UN) and hematite (Hem) in diopside matrix (Di). Transmitted light, parallel polars.

2019). Thermal metamorphic processes, initiated and maintained by one or more as yet poorly defined heat sources, resulted in temperatures up to 1400 °C at a near-atmospheric pressure (e.g. Vapnik et al., 2007). These P – T (pressure–temperature) conditions led to calcination and even fusion of sedimentary strata – chalks, marls and limestones – to form a variety of metamorphic lithologies, from marbles to the so-called “paralavas” (Vapnik et al., 2007). The 300 km² Daba-Siwaqa complex in central Jordan is a largest representative of the Hatrurim Formation (Abzalov et al., 2015; Vereshchagin et al., 2024b). The numerous abandoned quarries formerly operated for building stone expose the whole palette of fresh pyrometamorphic rocks. Moabite-bearing assemblages were found in a small quarry (31°21'52'' N, 36°10'55'' E), within the blocks of veined anorthite–diopside paralava, whose assemblages were previously described in detail (Britvin et al., 2023a; Vereshchagin et al., 2024b). Moabite is an accessory phase in these assemblages, where it associates with diopside; anorthite; native iron; hematite; and a series of recently discovered phosphides and phosphates – negevite, NiP_2 ; murashkoite, FeP ; transjordanite, Ni_2P ; halamishite, Ni_5P_4 ; crocobelonite, $\text{CaFe}_2^{3+}(\text{PO}_4)_2\text{O}$; yakubovichite, $\text{CaNi}_2\text{Fe}^{3+}(\text{PO}_4)_3$; and an alluaudite-group phosphate whose composition is exactly midway be-

Table 3. Chemical composition of moabite (wt %).

Constituent	Mean of five	Range
MgO	0.45	0.36–0.61
NiO	29.75	29.37–30.11
CuO	1.73	1.58–1.92
Fe_2O_3	36.04	34.70–37.11
Al_2O_3	0.19	0.00–0.38
V_2O_5	0.47	0.42–0.51
Cr_2O_3	0.18	0.00–0.32
P_2O_5	31.22	30.47–32.55
Total	100.03	

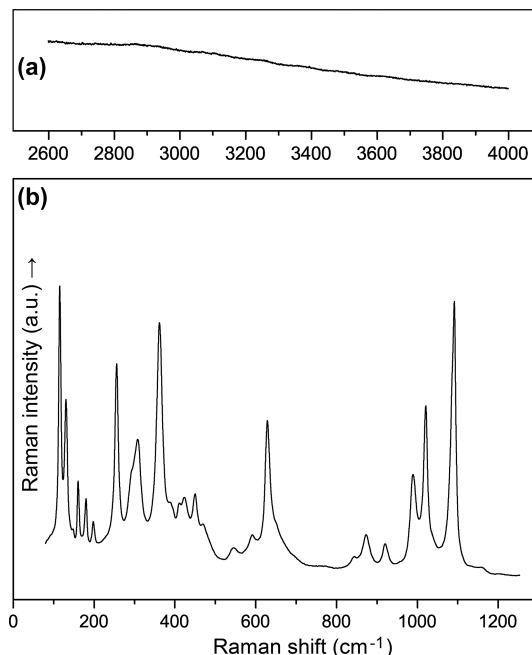
tween the two endmembers $\text{NaNaCa}(\text{Fe}^{3+}\text{Mg})(\text{PO}_4)_3$ and $\text{NaCa}(\text{Fe}^{3+}\text{Fe}^{3+})(\text{PO}_4)_3$. The relationships between the minerals indicate that moabite is the earliest phosphate but formed after hematite, iron and phosphide minerals.

4 Appearance and physical and optical properties

Moabite forms isometric to short prismatic crystals (Fig. 2a) and anhedral grains (Fig. 2b) up to 30 µm in size disseminated in a fine-grained matrix of anorthite–diopside paralava. The mineral often intergrows with other phosphates (Fig. 1b). Macroscopically, moabite has very dark-brown, almost-black, colour with vitreous lustre. In the thin sections in transmitted light, the mineral is semi-transparent with a red-brown colour. Due to the very high predicted value of the mean refractive index, 1.99, determination of refractive indices in transmitted light was considered impractical. In reflected light, the mineral has a grey colour with red-brown internal reflections. It is non-pleochroic, with weak anisotropy and bireflectance. Reflectance values are presented in Table 2.

5 Raman spectroscopy

The Raman spectrum of moabite (Fig. 3) contains the following bands (cm^{-1}): 115, 130, 160, 179, 198, 255, 292sh, 307, 361 and 388 (internal vibrations of $[\text{MO}_6]$ octahedra and lattice modes); 410, 423, 449 and 469 [ν_2 (symmetric bending vibrations of (PO_4) tetrahedra)]; 545, 590, 628 and 650sh [ν_4 (asymmetric bending vibrations of (PO_4) tetrahedra)]; 843, 871 and 918 [ν_1 (symmetric stretching modes of P–O bonds)]; and 988, 1019, 1090 and 1157 [ν_3 (asymmetric stretching vibrations of P–O)]. The band assignments were made based on the data previously reported for $\alpha\text{-Fe}_2\text{PO}_5$ (Wu et al., 2018) and $\text{CoIn}(\text{PO}_4)\text{O}$ (El Arni et al., 2023). The absence of bands in the region of stretching vibrations of O–H bonds ($3800\text{--}2800\text{ cm}^{-1}$) and bending modes of H_2O at $1600\text{--}1650\text{ cm}^{-1}$ provides evidence of the absence of water in the chemical composition of moabite.

**Figure 3.** Raman spectrum of moabite.

6 Chemical composition

Moabite crystals and grains have rather uniform chemical composition, with no zoning. Among the non-essential elements substituting for Ni and Fe, one can mention Cu, which was not previously detected in phosphates of the Hatrurim Formation. The Raman spectrum, the results of the structural study and bond-valence calculations are consistent with the absence of water in the composition of the mineral. Consequently, the average results of microprobe analyses (Table 3) can be calculated on the basis of 5 oxygen atoms per formula unit (apfu), yielding the empirical formula $(\text{Ni}_{0.90}\text{Cu}_{0.05}\text{Mg}_{0.03})_{\Sigma 0.98}(\text{Fe}^{3+}_{1.01}\text{Al}_{0.01}\text{Cr}_{0.01})_{\Sigma 1.03}(\text{P}_{0.99}\text{V}^{5+}_{0.01})_{\Sigma 1.00}\text{O}_5$, which corresponds to the ideal $\text{NiFe}^{3+}(\text{PO}_4)\text{O}$.

7 X-ray powder diffraction and crystal structure

Indexing of X-ray powder diffraction data for moabite (Table 4) and refinement of the unit-cell parameters (orthorhombic system, space group $Pnma$) give the following results: $a = 7.2145(3)$, $b = 6.4031(3)$, $c = 7.4657(3)$ Å and $V = 344.88(2)$ Å³. These parameters are consistent with the results obtained by the single-crystal study, which are provided in Table 5 along with the basic parameters of single-crystal data collection and structure refinement. Fractional atomic coordinates and displacement parameters for moabite are presented in Tables 6 and 7.

Moabite has a synthetic analogue, $\text{NiFe}^{3+}(\text{PO}_4)\text{O}$ (El Khayati et al., 2001); both crystallize in the $\alpha\text{-Fe}_2\text{PO}_5$ struc-

Table 4. X-ray powder diffraction data for moabite.

<i>I</i> _{meas}	<i>d</i> _{meas}	<i>I</i> _{calc}	<i>d</i> _{calc}	<i>hkl</i>	<i>I</i> _{meas}	<i>d</i> _{meas}	<i>I</i> _{calc}	<i>d</i> _{calc}	<i>hkl</i>
63	5.20	52	5.19	101	1	1.7537	2	1.7536	401
15	4.87	12	4.86	011	1	1.7376	1	1.7401	114
5	4.04	3	4.03	111			1	1.7365	410
17	3.609	18	3.608	200	3	1.7094	5	1.7100	322
37	3.321	31	3.317	102	1	1.6606	3	1.6586	204
83	3.251	91	3.249	201	2	1.6486	4	1.6489	232
16	3.207	13	3.203	020	15	1.6227	26	1.6245	402
3	3.133	1	3.143	210	5	1.6136	7	1.6134	024
11	2.948	8	2.946	112	15	1.6015	11	1.6057	214
1	2.915	1	2.898	211			21	1.6016	040
100	2.7262	100	2.7259	121	9	1.5715	5	1.5745	124
37	2.5946	33	2.5951	202			15	1.5719	420
16	2.4318	17	2.4316	022	1	1.5284	3	1.5304	141
19	2.3950	20	2.3954	220	18	1.5217	35	1.5222	323
25	2.3542	24	2.3540	103	5	1.4725	8	1.4729	224
12	2.3213	9	2.3210	013	2	1.4627	2	1.4639	240
24	2.3044	27	2.3043	122			1	1.4631	105
13	2.2866	13	2.2896	301	2	1.4413	5	1.4423	142
		8	2.2810	221	2	1.4356	6	1.4365	241
4	2.2106	6	2.2095	113	1	1.4246	2	1.4264	115
2	2.1556	3	2.1560	311			1	1.4244	413
18	2.0495	10	2.0532	031	1	1.4160	5	1.4170	501
		11	2.0495	203	3	1.3623	7	1.3629	242
12	2.0159	14	2.0164	222	1	1.3545	3	1.3552	431
1	1.9739	1	1.9748	131	4	1.3304	11	1.3308	125
5	1.8964	6	1.8969	123	3	1.3238	9	1.3242	143
14	1.8640	9	1.8676	004	6	1.3101	5	1.3124	341
		14	1.8627	321			12	1.3099	234
3	1.8361	4	1.8377	230	2	1.2957	2	1.2975	404
1	1.8092	2	1.8081	104			2	1.2959	521
1	1.8055	2	1.8040	400	2	1.2672	3	1.2692	305
2	1.7968	2	1.7956	132			1	1.2677	225

The measured intensities of the seven strongest lines are highlighted in bold. The theoretical pattern was calculated on the basis of atomic coordinates obtained from structure refinement and unit-cell parameters refined from powder data. Calculated lines with an intensity of less than 1 have been omitted.

ture type (Modaressi et al., 1983; Chemseddine and El Haibi, 1999). The mineral and synthetic compounds exhibit almost identical bond-valence sums (Table 8), providing evidence for the proper assignment of the metal oxidation states in moabite. Moabite is the first mineral that adopts the α -Fe₂PO₅ structure type (Table 9). Synthetic orthorhombic α -Fe₂PO₅ \equiv Fe²⁺Fe³⁺(PO₄)O, the structural prototype and Fe²⁺ analogue of moabite, is a high-temperature polymorph of Fe₂PO₅. Its low-temperature modification, β -Fe₂PO₅, adopts monoclinic (distorted-tetragonal) symmetry (Ech-Chahed et al., 1988; Ijjaali et al., 1990; Elkaïm et al., 1996). The crystal structure of the mineral consists of zigzag chains of alternating octahedra of [NiO₆] and [FeO₆] connected via the common faces, where [FeO₆] octahedra are located at the bends of the chains (Fig. 4). The oxide chains, propagated along the *b* axis, are linked both through the ex-

ternal corners of the [FeO₆] octahedra and via the corners of the [PO₄] tetrahedra.

Moabite is isotypic to transition metal oxyphosphates of the general formula $A^{2+}B^{3+}(PO_4)_O$ [$\equiv A^{2+}B^{3+}OPO_4$], where A^{2+} = Fe, Ni, Co and Cu and B^{3+} = Fe, V and In, which are extensively studied due to their magnetic and electrochemical properties (Ech-Chahed et al., 1988; El Khayati et al., 2001; Aziam et al., 2018, 2020; El Arni et al., 2023). There are two known oxyphosphate minerals with the stoichiometry M_2PO_5 : staněkite, Mn²⁺Fe³⁺(PO₄)O (Keller et al., 1997), and joosteite, Mn²⁺Mn³⁺(PO₄)O (Keller et al., 2007a) (Table 9). These minerals have crystal structures different from moabite and synthetic M_2PO_5 oxyphosphates.

Table 5. Crystal parameters, data collection and structure refinement details for moabite.

Crystal data	
Formula	NiFe(PO ₄)O
Crystal size (mm)	0.03 × 0.01 × 0.01
Crystal system	Orthorhombic
Space group	<i>Pnma</i>
<i>a</i> (Å)	7.2161(16)
<i>b</i> (Å)	6.4064(15)
<i>c</i> (Å)	7.4706(19)
<i>V</i> (Å ³)	345.4(1)
<i>Z</i>	4
<i>D_x</i> (g cm ⁻³)	4.338
Data collection and refinement	
Radiation	MoK α ($\lambda = 0.71073$ Å)
2 Θ range (°)	4.00–58.00
Total reflections collected	1866
No. of unique reflections	499
No. of unique observations, $I > 2\sigma(I)$	389
<i>h, k, l</i> range	−8 → 9, −8 → 7, −9 → 10
<i>F</i> (000)	436
μ (mm ⁻¹)	10.00
<i>R</i> _{int}	0.062
<i>R</i> ₁ [$F \geq 4\sigma(F)$]	0.033
<i>wR</i> ₂	0.071
<i>S</i> = GoF	1.04
Residual density (e Å ^{−3}) (min, max)	−0.90, 0.86

Table 6. Fractional atomic coordinates and isotropic displacement parameters (U_{iso} , Å²) for moabite.

Site	<i>x</i>	<i>y</i>	<i>z</i>	U_{iso}
Ni1 (4 <i>a</i>)	0	0	0	0.0060(2)
Fe1 (4 <i>c</i>)	0.14608(13)	1/4	0.70904(14)	0.0055(2)
P1 (4 <i>c</i>)	0.3725(2)	1/4	0.1410(2)	0.0042(4)
O1 (4 <i>c</i>)	0.3993(6)	1/4	0.6467(6)	0.0052(10)
O2 (4 <i>c</i>)	0.1951(6)	1/4	0.0233(7)	0.0075(11)
O3 (4 <i>c</i>)	0.0450(6)	1/4	0.4737(7)	0.0100(11)
O4 (8 <i>d</i>)	0.3682(4)	0.0574(5)	0.2642(4)	0.0074(7)

Note: Crystallographic tables were created using the PublICIF software (Westrip, 2010). Site multiplicities and Wyckoff symbols are given in parentheses.

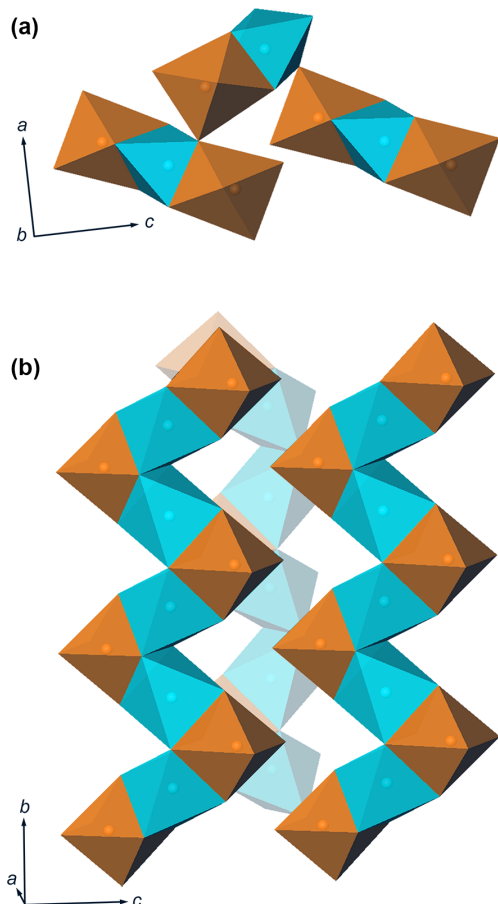
8 Discussion and conclusions

Moabite, which was discovered in pyrometamorphic assemblages, is a product of high-temperature pyrolytic oxidation of natural iron–nickel phosphides, as shown for crocobelonite, CaFe₂³⁺(PO₄)₂O (Britvin et al., 2023a). Phosphide assemblages are the typical feature of the Hatrurim Formation; they are known from several localities across Israel, Palestine and Jordan (Britvin et al., 2015, 2020a; Galuskin et al., 2023a). It is noteworthy that rare phosphide findings were also reported from other localities of pyrometamorphic origin (Savina et al., 2020). In addition,

natural phosphides occur in terrestrial basaltic iron assemblages (Klöck et al., 1986; Ulff-Møller, 1990; Vereshchagin et al., 2024a); they were found in coal-burnt dumps (Nishanbaev et al., 2002), mantle lithologies (Yang et al., 2005), fulgurites (Pasek and Block, 2009; Plyashkevich et al., 2016) and seabed sediments (Borodaev et al., 1982). Not all of these occurrences are suitable for postformational oxidation of phosphides, yet pyrometamorphism appears to present the most variable redox conditions. Phosphides, such as murashkoite, FeP; transjordanite–barringerite series, Ni₂P–Fe₂P; zuktamurrite, FeP₂; negevite, NiP₂; schreibersite, (Fe,Ni)₃P; and others (Britvin et al.,

Table 7. Anisotropic displacement parameters (\AA^2) for moabite.

Site	U^{11}	U^{22}	U^{33}	U^{12}	U^{13}	U^{23}
Ni1	0.0057(4)	0.0059(4)	0.0063(4)	-0.0004(4)	0.0004(4)	0.0007(4)
Fe1	0.0040(5)	0.0043(5)	0.0083(5)	0	0.0006(4)	0
P1	0.0014(8)	0.0051(9)	0.0062(8)	0	0.0002(7)	0
O1	0.004(2)	0.002(2)	0.009(2)	0	-0.0006(19)	0
O2	0.005(2)	0.005(2)	0.013(3)	0	-0.0044(19)	0
O3	0.003(2)	0.013(3)	0.014(3)	0	-0.002(2)	0
O4	0.0079(17)	0.0065(18)	0.0076(17)	-0.0005(13)	-0.0024(14)	0.0009(13)

**Figure 4.** Zigzag chains of octahedra [NiO₆] (blue) and [FeO₆] (brown) in the crystal structure of moabite. The octahedra within the chains are connected via alternation of common edges and faces. The chains are propagated along the b axis and linked by [PO₄] tetrahedra (not shown for clarity).

2020c; Galuskin et al., 2023a), are frequently associated with native iron, forming a fruitful basement for high-temperature oxidative transformations. In the case of oxidation alone, pure Fe–Ni phosphates are being formed, according to e.g. the following scheme: 2(FeNi)P (barringerite–transjordanite) + 5O₂ → 2FeNi(PO₄)O (moabite).

Table 8. Selected bond length (\AA) and bond-valence sum (BVS; v.u., valence unit) values for cationic sites of moabite and synthetic NiFe(PO₄)O*.

Bond	Moabite	NiFe(PO ₄)O
Ni1–O1	2.072(3) × 2	2.067(3) × 2
Ni1–O2	2.139(3) × 2	2.130(3) × 2
Ni1–O4	2.036(3) × 2	2.043(3) × 2
< Ni1–O >	2.082	2.080
BVS(Ni1)	2.07	1.91
Fe1–O1	2.081(5)	2.079(4)
Fe1–O1	1.886(5)	1.887(4)
Fe1–O2	2.374(5)	2.406(4)
Fe1–O3	1.903(5)	1.899(4)
Fe1–O4	2.014(3) × 2	2.006(2) × 2
< Fe1–O >	2.045	2.047
BVS(Fe1)	3.04	3.01
P1–O2	1.554(5)	1.549(6)
P1–O3	1.511(5)	1.506(6)
P1–O4	1.540(3) × 2	1.532(4) × 2
< P1–O >	1.536	1.530
BVS(P1)	5.08	5.06

* Bond-valence sums for moabite were calculated using microprobe-determined site populations normalized to 1, and bond-valence parameters were derived by Gagné and Hawthorne (2015). Bond-valence sums for synthetic NiFe(PO₄)O were taken from El Khayati et al. (2001).

In general, however, side reactions with the surrounding Ca-bearing silicates do occur, resulting in formation of more common Ca–Fe-bearing phosphates and oxyphosphates (Britvin et al., 2023a). The oxidation state of Ni in phosphates reaches Ni²⁺, whereas Fe state may vary between Fe²⁺ and Fe³⁺, depending on the local redox environment (Britvin et al., 2021d, 2023a).

Moabite, a Fe–Ni oxyphosphate, is a potential candidate for the occurrence in iron and stony-iron meteorites, where it could be formed by the oxidation of Fe–Ni metal–phosphide assemblages during high-temperature ablation processes. The recent discovery of ablation-formed iron oxyphosphates in the El Ali iron meteorite (Herd et al., 2024) shows that

Table 9. Crystallographic data for moabite and some related phosphates.

	Moabite	Synthetic	Synthetic	Synthetic	Staněkite- <i>Mabc</i>	Joosteite
Formula	NiFe(PO ₄)O	NiFe(PO ₄)O	α -Fe ₂ (PO ₄)O	β -Fe ₂ (PO ₄)O	MnFe(PO ₄)O	MnMn(PO ₄)O
Crystal system	Orthorhombic	Orthorhombic	Orthorhombic	Monoclinic	Monoclinic	Monoclinic
Space group	<i>Pnma</i>	<i>Pnma</i>	<i>Pnma</i>	<i>I2/a</i>	<i>P2₁/a</i>	<i>I2/a</i>
<i>a</i> (Å)	7.216	7.188	7.378	7.296	11.835	11.888
<i>b</i> (Å)	6.406	6.392	6.445	7.561	6.328	6.409
<i>c</i> (Å)	7.471	7.485	7.471	7.251	9.983	9.804
β (°)				117.4	105.81	106.17
<i>Z</i>	4	4	4	4	8	8
<i>V/Z</i> (Å ³)	86.4	86.0	88.8	88.8	89.9	89.7
Reference*	(1)	(2)	(3)	(4)	(5)	(6)

* References are as follows. (1) This work. (2) El Khayati et al. (2001). (3) Modaressi et al. (1981). (4) Elkaïm et al. (1996). (5) Keller et al. (2006). (6) Keller et al. (2007b).

ablation-formed phosphates deserve further investigation, with the possibility of the recognition of new mineral phases.

Data availability. The CIF file is available in the Supplement.

Supplement. The supplement related to this article is available online at <https://doi.org/10.5194/ejm-37-353-2025-supplement>.

Author contributions. MNM and YV found the specimens containing the mineral. SNB recognized the mineral in the samples, calculated the solution and performed the refinement of its crystal structure, interpreted the Raman spectrum, and wrote the manuscript. MGK processed X-ray powder diffraction data. NSV and OSV carried out electron microprobe analyses. DVP obtained the Raman spectrum. EAV collected the optical reflectance spectrum.

Competing interests. The contact author has declared that none of the authors has any competing interests.

Disclaimer. Publisher's note: Copernicus Publications remains neutral with regard to jurisdictional claims made in the text, published maps, institutional affiliations, or any other geographical representation in this paper. While Copernicus Publications makes every effort to include appropriate place names, the final responsibility lies with the authors.

Acknowledgements. The authors thank Ian Grey and the anonymous reviewer for their constructive comments and suggestions that improved the quality of the paper. The studies were carried out with instrumental and computational support of the Resource Centre for X-ray Diffraction Studies and Centre for Geo-Environmental Research and Modelling (GEOMODEL) of Saint Petersburg State University.

Financial support. This research has been supported by the Russian Science Foundation (grant no. 23-77-10025).

Review statement. This paper was edited by Sergey Krivovichev and reviewed by Ian Grey and one anonymous referee.

References

- Abzalov, M. Z., Van Der Heyden, A., Saymeh, A., and Abuqudaira, M.: Geology and metallogenesis of Jordanian uranium deposits, *Appl. Earth Sci. Trans. Inst. Min.*, 124, 63–77, <https://doi.org/10.1179/1743275815Y.0000000009>, 2015.
- Aziam, H., Garhi, G., Tamraoui, Y., Ma, L., Wu, T., Xu, G. L., Manoun, B., Alami, J., Amine, K., and Saadoune, I.: Understanding the electrochemical lithiation / delithiation process in the anode material for lithium ion batteries NiFeOPO₄ / C using ex-situ X-ray absorption near edge spectroscopy and in-situ synchrotron X-ray, *Electrochim. Ac.*, 283, 1238–1244, <https://doi.org/10.1016/j.electacta.2018.07.038>, 2018.
- Aziam, H., Youcef, H. B., and Saadoune, I.: Evidence of CoFeOPO₄ activity in Na-ion batteries, *J. Electroanal. Chem.*, 874, 114450, <https://doi.org/10.1016/j.jelechem.2020.114450>, 2020.
- Ben-Avraham, Z., Garfunkel, Z., and Lazar, M.: Geology and evolution of the Southern Dead Sea Fault with emphasis on subsurface structure, *Ann. Rev. Earth Planet. Sci.*, 36, 357–387, <https://doi.org/10.1146/annurev.earth.36.031207.124201>, 2008.
- Borodaev, Y. S., Bogdanov, Y. A., and Vyalsov, L. N.: New nickel-free variety of schreibersite Fe₃P, *Proc. All-Union Mineral. Soc.*, 111, 682–687, 1982 (in Russian).
- Britvin, S. N., Murashko, M. N., Vapnik, Y., Polekhovsky, Y. S., and Krivovichev, S. V.: Earth's Phosphides in Levant and insights into the source of Archean prebiotic phosphorus, *Sci. Rep.*, 5, 8355, <https://doi.org/10.1038/srep08355>, 2015.
- Britvin, S. N., Dolivo-Dobrovolsky, D. V., and Krzhizhanovskaya, M. G.: Software for processing the X-ray powder diffraction data obtained from the curved image plate detector of Rigaku RAXIS Rapid II diffractometer, *Zap. Ross. Mineral. Obshch.*, 146, 104–107, 2017 (in Russian).

- Britvin, S. N., Murashko, M. N., Vapnik, Ye., Polekhovsky, Yu. S., Krivovichev, S. V., Krzhizhanovskaya, M. G., Vereshchagin, O. S., Shilovskikh, V. V., and Vlasenko, N. S.: Transjordanite, Ni₂P, a new terrestrial and meteoritic phosphide, and natural solid solutions barringerite–transjordanite (hexagonal Fe₂P–Ni₂P). *Am. Mineral.*, 105, 428–436, <https://doi.org/10.2138/am-2020-7275>, 2020a.
- Britvin, S. N., Murashko, M. N., Vapnik, Ye., Polekhovsky, Yu. S., Krivovichev, S. V., Vereshchagin, O. S., Shilovskikh, V. V., Vlasenko, N. S., and Krzhizhanovskaya, M. G.: Halamishite, Ni₅P₄, a new terrestrial phosphide in the Ni-P system. *Phys. Chem. Miner.*, 47, 3, <https://doi.org/10.1007/s00269-019-01073-7>, 2020b.
- Britvin, S. N., Murashko, M. N., Vapnik, Ye., Polekhovsky, Yu. S., Krivovichev, S. V., Vereshchagin, O. S., Shilovskikh, V. V., and Krzhizhanovskaya, M. G.: Negevite, the pyrite-type NiP₂, a new terrestrial phosphide, *Am. Mineral.*, 105, 422–427, <https://doi.org/10.2138/am-2020-7192>, 2020c.
- Britvin, S. N., Vereshchagin, O. S., Shilovskikh, V. V., Krzhizhanovskaya, M. G., Gorelova, L. A., Vlasenko, N. S., Pakhomova, A. S., Zaitsev, A. N., Zolotarev, A. A., Bykov, M., Lozhkin, M. S., and Nestola, F.: Discovery of terrestrial allabogdanite (Fe, Ni)₂P, and the effect of Ni and Mo substitution on the barringerite-allabogdanite high-pressure transition, *Am. Mineral.*, 106, 944–952, <https://doi.org/10.2138/am-2021-7621>, 2021a.
- Britvin, S. N., Krzhizhanovskaya, M. G., Zolotarev, A. A., Gorelova, L. A., Obolonskaya, E. V., Vlasenko, N. S., Shilovskikh, V. V., and Murashko, M. N.: Crystal chemistry of schreibersite, (Fe, Ni)₃P, *Am. Mineral.*, 106, 1520–1529, <https://doi.org/10.2138/am-2021-7766>, 2021b.
- Britvin, S. N., Galuska, I. O., Vlasenko, N. S., Vereshchagin, O. S., Bocharov, V. N., Krzhizhanovskaya, M. G., Shilovskikh, V. V., Galuska, I. O., Vapnik, Y., and Obolonskaya, E. V.: Kepplerite, Ca₉(Ca_{0.5}□_{0.5})Mg(PO₄)₇, a new meteoritic and terrestrial phosphate isomorphous with merrillite, Ca₉NaMg(PO₄)₇, *Am. Mineral.*, 106, 1917–1927, <https://doi.org/10.2138/am-2021-7834>, 2021c.
- Britvin, S. N., Murashko, M. N., Vapnik, Ye., Vlasenko, N. S., Krzhizhanovskaya, M. G., Vereshchagin, O. S., Bocharov, V. N., and Lozhkin, M. S.: Cyclophosphates, a new class of native phosphorus compounds, and some insights into prebiotic phosphorylation on early Earth, *Geology*, 49, 382–386, <https://doi.org/10.1130/G48203.1>, 2021d.
- Britvin, S. N., Murashko, M. N., Vapnik, Ye., Zaitsev, A. N., Shilovskikh, V. V., Krzhizhanovskaya, M. G., Gorelova, L. A., Vereshchagin, O. S., Vasilev, E. A., and Vlasenko, N. S.: Orishchinit, a new terrestrial phosphide, the Ni-dominant analogue of allabogdanite, *Mineral. Petrol.*, 116, 369–378, <https://doi.org/10.1007/s00710-022-00787-x>, 2022a.
- Britvin, S. N., Vlasenko, N. S., Aslandukov, A., Aslandukova, A., Dubrovinsky, L., Gorelova, L. A., Krzhizhanovskaya, M. G., Vereshchagin, O. S., Bocharov, V. N., Shelukhina, Yu. S., Lozhkin, M. S., Zaitsev, A. N., and Nestola, F.: Natural cubic perovskite, Ca(Ti,Si,Cr)O_{3-δ}, a versatile potential host for rock-forming and less common elements up to Earth's mantle pressure, *Am. Mineral.*, 107, 1936–1945, <https://doi.org/10.2138/am-2022-8186>, 2022b.
- Britvin, S. N., Murashko, M. N., Krzhizhanovskaya, M. G., Vereshchagin, O. S., Vapnik, Ye., Shilovskikh, V. V., Lozhkin, M. S., and Obolonskaya, E. V.: Nazarovite, Ni₁₂P₅, a new terrestrial and meteoritic mineral structurally related to nickelphosphide, Ni₃P, *Am. Mineral.*, 107, 1946–1951, <https://doi.org/10.2138/am-2022-8219>, 2022c.
- Britvin, S. N., Murashko, M. N., Vereshchagin, O. S., Vapnik, Ye., Shilovskikh, V. V., Vlasenko, N. S., and Permyakov, V. V.: Expanding the speciation of terrestrial molybdenum: Discovery of polekhovskyite, MoNiP₂, and insights into the sources of Mophosphides in the Dead Sea Transform area, *Am. Mineral.*, 107, 2201–2211, <https://doi.org/10.2138/am-2022-8261>, 2022d.
- Britvin, S. N., Murashko, M. N., Krzhizhanovskaya, M. G., Vlasenko, N. S., Vereshchagin, O. S., Vapnik, Y., and Bocharov, V. N.: Crocobelonite, CaFe³⁺₂(PO₄)₂O, a new oxyphosphate mineral, the product of pyrolytic oxidation of natural phosphides, *Am. Mineral.*, 108, 1973–1983, <https://doi.org/10.2138/am-2022-8757>, 2023a.
- Britvin, S. N., Murashko, M. N., Krzhizhanovskaya, M. G., Vapnik, Ye., Vlasenko, N. S., Vereshchagin, O. S., Pankin, D. V., Zaitsev, A. N., and Zolotarev, A. A.: Yakubovichite, CaNi₂Fe³⁺₂(PO₄)₃, a new nickel phosphate mineral of non-meteoritic origin, *Am. Mineral.*, 108, 2142–2150, <https://doi.org/10.2138/am-2022-8800>, 2023b.
- Burg, A., Starinsky, A., Bartov, Y., and Kolodny, Y.: Geology of the Hatrurim Formation (“Mottled Zone”) in the Hatrurim basin, *Isr. J. Earth Sci.*, 40, 107–124, 1992.
- Chemseddine, E. and El Hajbi, A.: Application of the alternating spin chain model to the α-Fe₂PO₅ compound, *Ann. Chim. Sci. Matér.*, 24, 241–244, [https://doi.org/10.1016/S0151-9107\(99\)80050-6](https://doi.org/10.1016/S0151-9107(99)80050-6), 1999.
- Cipriani, C., Mellini, M., Pratesi, G., and Viti, C.: Rodolicoite and grattarolite, two new phosphate minerals from Santa Barbara Mine, Italy, *Eur. J. Mineral.*, 9, 1101–1106, <https://doi.org/10.1127/ejm/9/5/1101>, 1997.
- Dolomanov, O. V., Bourhis, L. J., Gildea, R. J., Howard, J. A., and Puschmann, H.: OLEX2: a complete structure solution, refinement and analysis program, *J. Appl. Cryst.*, 42, 339–341, <https://doi.org/10.1107/S0021889808042726>, 2009.
- Ech-Chahed, B., Jeannot, F., Malaman, B., and Gleitzer, C.: Préparation et étude d'une variété basse température de l'oxyphosphate de fer de valence mixte βFe₂(PO₄)O et de NiCr(PO₄)O: Un cas d'échangeélectronique rapide, *J. Solid State Chem.*, 74, 47–59, [https://doi.org/10.1016/0022-4596\(88\)90330-1](https://doi.org/10.1016/0022-4596(88)90330-1), 1988.
- Elkaïm, E., Berar, J. F., Gleitzer, C., Malaman, B., Ijjaali, M., and Lecomte, C.: Occurrence of a monoclinic distortion in β-Fe₂PO₅, *Acta Crystallogr. B*, 52, 428–431, <https://doi.org/10.1107/S0108768195014273>, 1996.
- El Arni, S., Rguig, O., Hadouchi, M., Assani, A., Saadi, M., Lahmar, A., Bouyanif, H., El Marssi, M., and El Amari, L.: Synthesis, structural characterization and magnetic properties of CoInOPO₄ with the α-Fe₂OPO₄ structure, *J. Solid State Chem.*, 324, 124111, <https://doi.org/10.1016/j.jssc.2023.124111>, 2023.
- El Khayati, N., Cherkaoui El Moursli, R., Rodríguez-Carvajal, J., André, G., Blanchard, N., Bourée, F., Collin, G., and Roisnel, T.: Crystal and magnetic structures of the oxophosphates MFePO₅ (M = Fe, Co, Ni, Cu), Analysis of the magnetic ground state in terms of superexchange interactions, *Eur. Phys. J. B*, 22, 429–442, <https://doi.org/10.1007/s100510170093>, 2001.

- Finkelstein, I. and Lipschits, O.: The genesis of Moab: a proposal, Levant, 43, 139–152, <https://doi.org/10.1179/175638011X13112549593005>, 2011.
- Fleurance, S., Cuney, M., Malartre, M., and Reyx, J.: Origin of the extreme polymetallic enrichment (Cd, Cr, Mo, Ni, U, V, Zn) of the Late Cretaceous–Early Tertiary Belqa Group, central Jordan, Palaeogeogr. Palaeoecol., 369, 201–219, <https://doi.org/10.1016/j.palaeo.2012.10.020>, 2013.
- Gagné, O. C. and Hawthorne, F. C.: Comprehensive derivation of bond-valence parameters for ion pairs involving oxygen, Acta Crystallogr. B, 71, 562–578, <https://doi.org/10.1107/S2052520615016297>, 2015.
- Galuskin, E. V., Gfeller, F., Galuskina, I. O., Pakhomova, A., Armbruster, T., Vapnik, Y., Włodyka, R., Dzierżanowski, P., and Murashko, M.: New minerals with a modular structure derived from hatrurite from the pyrometamorphic Hatrurim Complex, Part II, Zadovite, $\text{BaCa}_6[(\text{SiO}_4)(\text{PO}_4)](\text{PO}_4)_2\text{F}$ and aradite, $\text{BaCa}_6[(\text{SiO}_4)(\text{VO}_4)](\text{VO}_4)_2\text{F}$, from paralavas of the Hatrurim Basin, Mineral. Mag., 79, 1073–1087, <https://doi.org/10.1180/minmag.2015.079.5.04>, 2015.
- Galuskin, E. V., Galuskina, I. O., Gfeller, F., Krüger, B., Kusz, J., Vapnik, Y., Dulski, M., and Dzierżanowski, P.: Silicocarnotite, $\text{Ca}_5[(\text{SiO}_4)(\text{PO}_4)](\text{PO}_4)$, a new "old" mineral from the Negev Desert, Israel, and the ternesite–silicocarnotite solid solution: indicators of high-temperature alteration of pyrometamorphic rocks of the Hatrurim Complex, Southern Levant, Eur. J. Mineral., 28, 105–123, <https://doi.org/10.1127/ejm/2015/0027-2494>, 2016.
- Galuskin, E. V., Krüger, B., Galuskina, I. O., Krüger, H., Vapnik, Y., Pauluhn, A., and Olieric, V.: Strachterite, $\text{BaCa}_6(\text{SiO}_4)_2[(\text{PO}_4)(\text{CO}_3)]\text{F}$, the first CO_3 -bearing intercalated hexagonal antiperovskite from Negev Desert, Israel, Am. Mineral., 103, 1699–1706, <https://doi.org/10.2138/am-2018-6493>, 2018a.
- Galuskin, E. V., Krüger, B., Galuskina, I. O., Krüger, H., Vapnik, Y., Wojdyla, J. A., and Murashko, M.: New mineral with modular structure derived from hatrurite from the pyrometamorphic rocks of the Hatrurim Complex: Ariegilatite, $\text{BaCa}_{12}(\text{SiO}_4)_4(\text{PO}_4)_2\text{F}_2\text{O}$, from Negev Desert, Israel, Minerals, 8, 109, <https://doi.org/10.3390/min8030109>, 2018b.
- Galuskin, E. V., Krüger, B., Galuskina, I. O., Krüger, H., Vapnik, Y., Pauluhn, A., and Olieric, V.: Levantite, $\text{KCa}_3(\text{Al}_2\text{Si}_3\text{O}_{11})(\text{PO}_4)$, a new latiumite-group mineral from the pyrometamorphic rocks of the Hatrurim Basin, Negev Desert, Israel, Mineral. Mag., 83, 713–721, <https://doi.org/10.1180/mgm.2019.37>, 2019.
- Galuskin, E., Galuskina, I., Krüger, B., Krüger, H., Vapnik, Y., Krzatała, A., Środek, D., and Zieliński, G.: Nomenclature and Classification of the Arctite Supergroup, Aravaite, $\text{Ba}_2\text{Ca}_{18}(\text{SiO}_4)_6(\text{PO}_4)_3(\text{CO}_3)\text{F}_3\text{O}$, a New Arctite Supergroup Mineral from Negev Desert, Israel, Can. Mineral., 59, 191–209, <https://doi.org/10.3749/canmin.2000035>, 2021.
- Galuskin, E. V., Stachowicz, M., Galuskina, I. O., Wózniak, K., Vapnik, Y., Murashko, M. N., and Zieliński, G.: Deynekoite, $\text{Ca}_9\text{Fe}^{3+}(\text{PO}_4)_7$ – a new mineral of the merrillite group from phosphide-bearing contact facies of paralava, Hatrurim Complex, Daba-Siwaqa, Jordan, Mineral. Mag., 87, 943–954, <https://doi.org/10.1180/mgm.2023.71>, 2023a.
- Galuskin, E. V., Kusz, J., Galuskina, I. O., Książek, M., Vapnik, Ye., and Zieliński, G.: Discovery of terrestrial andreyivanovite, FeCrP, and the effect of Cr and V substitution on the low-pressure barringerite-allabogdanite transition, Am. Mineral., 108, 1506–1515, <https://doi.org/10.2138/am-2022-8647>, 2023b.
- Galuskin, E. V., Galuskina, I. O., Kusz, J., Książek, M., Vapnik, Y., and Zieliński, G.: Karwowskiite, $\text{Ca}_9(\text{Fe}_{0.5}^{2+}\square_{0.5})\text{Mg}(\text{PO}_4)_7$ – A New Merrillite Group Mineral from Paralava of the Hatrurim Complex, Daba-Siwaqa, Jordan, Minerals, 14, 825, <https://doi.org/10.3390/min14080825>, 2024.
- Gross, S.: The mineralogy of the Hatrurim Formation, Israel, Geol. Surv. Isr. Bull., 70, 1–80, 1977.
- Herd, C. D. K., Ma, C., Locock, A. J., Saini, R., and Walton, E. L.: Three new iron-phosphate minerals from the El Ali iron meteorite, Somalia: Elalite $\text{Fe}_8^{2+}\text{Fe}^{3+}(\text{PO}_4)_8$, elkinstantonite $\text{Fe}_4(\text{PO}_4)_2\text{O}$, and olsenite $\text{KFe}_4(\text{PO}_4)_3$, Am. Mineral., 109, 2142–2151, <https://doi.org/10.2138/am-2023-9225>, 2024.
- Ijjaali, M., Malaman, B., Gleitzer, C., Warner, J. K., Hriljac, J. A., and Cheetham, K. A.: Stability, structure refinement, and magnetic properties of $\beta\text{-Fe}_2(\text{PO}_4)\text{O}$, J. Solid State Chem., 86, 195–205, [https://doi.org/10.1016/0022-4596\(90\)90135-K](https://doi.org/10.1016/0022-4596(90)90135-K), 1990.
- Juroszek, R., Galuskina, I., Krüger, B., Krüger, H., Vapnik, Ye., Kahlenberg, V., and Galuskin, E.: Minerals with a palmierite-type structure. Part I. Mazorite $\text{Ba}_3(\text{PO}_4)_2$, a new mineral from the Hatrurim Complex in Israel, Mineral. Mag., 87, 679–689, <https://doi.org/10.1180/mgm.2023.57>, 2023.
- Keller, P., Fontan, F., Velasco-Roldan, F., and Melgarejo i Draper, J. C.: Staněkite, $\text{Fe}^{3+}(\text{Mn},\text{Fe}^{2+},\text{Mg})(\text{PO}_4)\text{O}$: a new phosphate mineral in pegmatites at Karibib (Namibia) and French Pyrenees (France), Eur. J. Mineral., 9, 475–482, <https://doi.org/10.1127/ejm/9/3/0475>, 1997.
- Keller, P., Lissner, F., and Schleid, T.: The crystal structure of staněkite, $(\text{Fe}^{3+}, \text{Mn}^{2+}, \text{Fe}^{2+}, \text{Mg})_2[\text{PO}_4]\text{O}$, from Okatjimukuju, Karibib (Namibia), and its relationship to the polymorphs of synthetic $\text{Fe}_2[\text{PO}_4]\text{O}$, Eur. J. Mineral., 18, 113–118, <https://doi.org/10.1127/0935-1221/2006/0018-0113>, 2006.
- Keller, P., Fontan, F., Roldan, F. V., and de Parseval, P.: Joosteite, $\text{Mn}^{2+}(\text{Mn}^{3+}, \text{Fe}^{3+})(\text{PO}_4)\text{O}$: a new phosphate mineral from the Helikon II Mine, Karibib, Namibia, N. Jahrb. Mineral. Abh., 183, 197–201, <https://doi.org/10.1127/0077-7757/2007/0069>, 2007a.
- Keller, P., Lissner, F., and Schleid, T.: The crystal structure of joosteite, $(\text{Mn}^{2+}, \text{Mn}^{3+}, \text{Fe}^{3+})_2(\text{PO}_4)\text{O}$, from the Helikon II Mine, Karibib (Namibia) and its relationship to staněkite, $(\text{Fe}^{3+}, \text{Mn}^{2+}, \text{Fe}^{2+}, \text{Mg})_2(\text{PO}_4)\text{O}$, N. Jahrb. Mineral. Abh., 184, 225–230, <https://doi.org/10.1127/0077-7757/2007/0095>, 2007b.
- Klöck, W., Palme, H., and Tobischall, H. J.: Trace elements in natural metallic iron from Disko Island, Greenland, Contrib. Mineral. Petrol., 93, 273–282, <https://doi.org/10.1007/BF00389387>, 1986.
- Krzatała, A., Skryńska, K., Cametti, G., Galuskina, I., Vapnik, Ye., and Galuskin, E.: Fluoralforsite, $\text{Ba}_5(\text{PO}_4)_3\text{F}$ – a new apatite-group mineral from the Hatrurim Basin, Negev Desert, Israel, Mineral. Mag., 87, 866–877, <https://doi.org/10.1180/mgm.2023.58>, 2023.
- Modaressi, A., Courtois, A., Gerardin, R., Malaman, B., and Gleitzer, C.: Fe_3PO_7 , Un cas de coordination 5 du fer trivalent, étude structurale et magnétique, J. Solid State Chem., 47, 245–255, [https://doi.org/10.1016/0022-4596\(83\)90016-6](https://doi.org/10.1016/0022-4596(83)90016-6), 1983.
- Murashko, M. N., Britvin, S. N., Vapnik, Ye., Polekhovsky, Y. S., Shilovskikh, V. V., Zaitsev, A. N., and Vereshchagin, O. S.: Nick-

- olayite, FeMoP, a new natural molybdenum phosphide, *Mineral. Mag.*, 86, 749–757, <https://doi.org/10.1180/mgm.2022.52>, 2022.
- Nishanbaev, T. P., Rochev, A. V., and Kotlyarov, V. A.: Iron phosphides from combustion dumps of Chelyabinsk coal basin, *Ural. Geol. J.*, 25, 105–114, 2002 (in Russian).
- Novikov, I., Vapnik, Ye., and Safonova, I.: Mud volcano origin of the Mottled Zone, Southern Levant, *Geosci. Front.*, 4, 597–619, <https://doi.org/10.1016/j.gsf.2013.02.005>, 2013.
- Pasek, M. and Block, K.: Lightning-induced reduction of phosphorus oxidation state, *Nat. Geosci.*, 2, 553–556, <https://doi.org/10.1038/ngeo580>, 2009.
- Plyashkevich, A. A., Minyuk, P. S., Subbotnikova, T. V., and Alshevsky, A. V.: Newly formed minerals of the Fe-P-S system in Kolymsky fulgurite, *Dokl. Earth Sci.*, 467, 380–383, <https://doi.org/10.1134/S1028334X16040139>, 2016.
- Savina, E. A., Peretyazhko, I. S., Khromova, E. A., and Glushkova, V. E.: Melted rocks (clinkers and paralavas) of Khamaryn-Khural-Khiid combustion metamorphic complex in Eastern Mongolia: Mineralogy, geochemistry and genesis, *Petrology*, 28, 431–457, <https://doi.org/10.1134/S0869591120050057>, 2020.
- Sheldrick, G. M.: Crystal structure refinement with SHELXL, *Acta Crystallogr. C*, 71, 3–8, <https://doi.org/10.1107/S2053229614024218>, 2015.
- Sokol, E. V., Novikov, I. S., Vapnik, Y., and Sharygin, V. V.: Gas fire from mud volcanoes as a trigger for the appearance of high-temperature pyrometamorphic rocks of the Hatrurim Formation (Dead Sea area), *Dokl. Earth Sci.*, 413, 474–480, <https://doi.org/10.1134/S1028334X07030348>, 2007.
- Sokol, E., Novikov, I., Zateeva, S., Vapnik, Ye., Shagam, R., and Kozmenko, O.: Combustion metamorphism in the Nabi Musa dome: New implications for a mud volcanic origin of the Mottled Zone, Dead Sea area, *Basin Res.*, 22, 414–438, <https://doi.org/10.1111/j.1365-2117.2010.00462.x>, 2010.
- Sokol, E. V., Kozmenko, O. A., Kokh, S. N., and Vapnik, Ye.: Gas reservoirs in the Dead Sea area: Evidence from chemistry of combustion metamorphic rocks in Nabi Musa fossil mud volcano, *Russ. Geol. Geophys.*, 53, 745–762, <https://doi.org/10.1016/j.rgg.2012.06.003>, 2012.
- Sokol, E. V., Seryotkin, Y. V., Kokh, S. N., Vapnik, Ye., Nigmatulina, E. N., Goryainov, S. V., Belogub, E. V., and Sharygin, V. V.: Flamite, (Ca,Na,K)₂(Si,P)O₄, a new mineral from ultrahigh-temperature combustion metamorphic rocks, Hatrurim Basin, Negev Desert, Israel, *Mineral. Mag.*, 79, 583–596, <https://doi.org/10.1180/minmag.2015.079.3.05>, 2015.
- Sokol, E. V., Kokh, S. N., Sharygin, V. V., Danilovsky, V. A., Seryotkin, Yu. V., Liferovich, R., Deviatiiarova, A. S., Nigmatulina, E. N., and Karmanov, N. S.: Mineralogical diversity of Ca₂SiO₄-bearing combustion metamorphic rocks in the Hatrurim Basin: Implications for storage and partitioning of elements in oil shale clinkering, *Minerals*, 9, 465, <https://doi.org/10.3390/min9080465>, 2019.
- Ulff-Møller, F.: Formation of native iron in sediment-contaminated magma. I. A case study of the Hanekammen Complex on Disko Island, West Greenland, *Geochim. Cosmochim. Ac.*, 54, 57–70, [https://doi.org/10.1016/0016-7037\(90\)90195-Q](https://doi.org/10.1016/0016-7037(90)90195-Q), 1990.
- Vapnik, Ye., Sharygin, V. V., Sokol, E. V., and Shagam, R.: Paralavas in a combustion metamorphic complex: Hatrurim Basin, Israel, *Geol. Soc. Am. Rev. Eng. Geol.*, 18, 133–153, [https://doi.org/10.1130/2007.4118\(09\)](https://doi.org/10.1130/2007.4118(09)), 2007.
- Vereshchagin, O. S., Khmelnietskaya, M. O., Kamaeva, L. V., Vlasenko, N. S., Pankin, D. V., Bocharov, V. N., and Britvin, S. N.: Telluric iron assemblages as a source of prebiotic phosphorus on the early Earth: Insights from Disko Island, Greenland, *Geosci. Front.*, 15, 101870, <https://doi.org/10.1016/j.gsf.2024.101870>, 2024a.
- Vereshchagin, O. S., Khmelnietskaya, M. O., Murashko, M. N., Vapnik, Ye., Zaitsev, A. N., Vlasenko, N. S., Shilovskikh, V. V., and Britvin, S. N.: Reduced mineral assemblages of superficial origin in west-central Jordan, *Mineral. Petrol.*, 118, 305–319, <https://doi.org/10.1007/s00710-024-00851-8>, 2024b.
- Westrip, S. P.: publCIF: Software for Editing, Validating and Formatting Crystallographic Information Files, *J. Appl. Cryst.*, 43, 920–925, <https://doi.org/10.1107/S0021889810022120>, 2010.
- Wu, Y. Z., Meng, Y. N., Hou, J. G., Cao, S., Gao, Z., Wu, Z., and Sun, L.: Orienting active crystal planes of new class lacunarite Fe₂PO₅ polyhedrons for robust water oxidation in alkaline and neutral media, *Adv. Funct. Mater.*, 28, 1801397, <https://doi.org/10.1002/adfm.201801397>, 2018.
- Yang, J. S., Bai, W. J., Rong, H., Zhang, Z. M., Xu, Z. Q., Fang, Q. S., Yang, B. G., Li, T. F., Ren, Y. F., Chen, S. Y., Hu, J.-Z., Su, J. F., and Mao, H. K.: Discovery of Fe₂P alloy in garnet peridotite from the Chinese continental scientific drilling project (CCSD) main hole, *Acta Petrol. Sin.*, 21, 271–276, 2005.